

## CONDITIONS OF THE FERROWOLLASTONITE-FERROHEDENBERGITE INVERSION IN THE SKAERGAARD INTRUSION, EAST GREENLAND

D. H. LINDSLEY

*Geophysical Laboratory, 2801 Upton Street, N.W., Washington, D.C. 20008*

G. MALCOLM BROWN, *Department of Geology, Durham University, South Road, Durham City, England*

AND

I. D. MUIR

*Department of Mineralogy and Petrology, Cambridge University, Downing Street, Cambridge, England*

### ABSTRACT

Rocks from the late stages of fractionation of the Skaergaard intrusion contain ferrohedenbergites inverted from ferro-wollastonite solid solutions (Upper Zone c) and quartz inverted from tridymite (Upper Border Group  $\gamma$ ). Experiments determining the pressure-temperature conditions of the hedenbergite-wollastonite solid-solution inversion for an analyzed Skaergaard ferrohedenbergite (EG 4471), combined with published data on the quartz-tridymite inversion, show that the pressure was  $600 \pm 100$  bars and that the temperature range included the span 980 to 950°C during the late stages of crystallization of the Skaergaard intrusion. The oxygen fugacity under these conditions is calculated to have ranged from  $10^{-13.9}$  to  $10^{-13.6}$  atm. These values are about one and one-half orders of magnitude below those of the fayalite-magnetite-quartz buffer, and essentially coincide with those of the wüstite-magnetite buffer.

The absence of inverted ferro-wollastonite solid solutions in the Bushveld intrusion is ascribed to higher pressure prevailing during the crystallization of that body relative to the Skaergaard intrusion.

### INTRODUCTION

The clinopyroxenes crystallized during the late stages of fractionation of the Skaergaard intrusion and of the Bushveld intrusion have closely similar compositional trend-lines (Wager and Brown, 1968, pp. 39; 391). A minor but significant difference between them is the presence in the Skaergaard intrusion of green hebenbergitic pyroxenes ( $Hd_{ss}$ ) that are believed to have inverted from ferrowollastonite solid solutions ( $Wo_{ss}$ ) Wager and Deer, 1939, p. 111; Muir, 1951, pp. 708–709, Brown and Vincent, 1963, pp. 186–190; Wager and Brown, 1968, pp. 41–42). Lindsley (1967, pp. 232–234) proposed that the absence of inverted  $Wo_{ss}$  from the Bushveld intrusion resulted from crystallization of that body at somewhat higher pressures than prevailed during the late crystallization stages of the Skaergaard intrusion. In this paper we report experiments on the  $Hd_{ss}$ - $Wo_{ss}$  inversion in several analyzed Mg-poor clinopyroxenes from the Skaergaard intrusion and one from the Bushveld intrusion. The pressure-dependence of the inversion temperature in one inverted  $Wo_{ss}$  (from Skaergaard sample EG 4471), combined with data in the quartz-tridymite inversion (Tuttle and Bowen, 1958, pp. 30–32) yields the temperature range and pressure that must have prevailed at some stage during crystallization of Upper Zone c (Fig. 1) of the Skaergaard intrusion. Thus it is possible to adduce data on some of the intensive parameters that controlled late-stage crystallization of that intrusion. Our results corroborate, but do not prove conclusively, the inference that the late stages of the Skaergaard intrusion crystallized at lower pressures than did the equivalent portions of the Bushveld intrusion.

### FIELD AND CHEMICAL DATA

The Upper Zone of the Skaergaard layered series of crystal accumulates consists of ferrodiorites showing progressive iron enrichment with height. The mineral assemblage of the Upper Zone consists of coexisting (cumulus) phases which show gradual compositional changes with layer-height (*i.e.*, crystallization stage), continuous with the solid solution changes in the minerals of underlying zones. Plagioclase changes from  $An_{45}$  to  $An_{30}$ , olivine from  $Fo_{40}$  to  $Fo_0$ , and ferroaugite from  $Ca_{35}Mg_{37}Fe_{28}$  to approximately  $Ca_{43}Mg_0Fe_{57}$ . Cumulus apatite and subordinate (often intercumulus) micropegmatite, Fe-Ti oxides, and sulfides occur within the zone (Wager and Brown, 1968, Fig. 14). The Upper Zone (UZ) is divided according to the entry of cumulus apatite (UZ b) and ferro-wollastonite (UZ c). The analyzed ferroaugites from these Upper Zone rocks plot on an extension of the regular trend shown by the augites analyzed from underlying zones, the complete trend ending very close to the  $CaSiO_3$ - $FeSiO_3$  edge of the common pyroxene quadrilateral (Fig. 2), with a ferrohedenbergite of composition  $Wo_{42.5}En_{0.4}Fs_{57.1}$  (mole %). This brown pyroxene occurs in the last demonstrable differentiate (EG 4330) of the intrusion and shown no textural evidence of inversion from a ferro-wollastonite. In rocks slightly lower in the Upper Zone layered series (Fig. 1) occur green ferrohedenbergites with the mosaic texture ascribed to inversion from ferro-wollastonites. The green ferrohedenbergite from Skaergaard specimen EG 4471 is the richest in ferrosilite of the pyroxenes reported by Brown and Vincent (1963, Fig. 3). Between the structural levels of EG 4471 and 4330, rocks such as EG 1881 con-

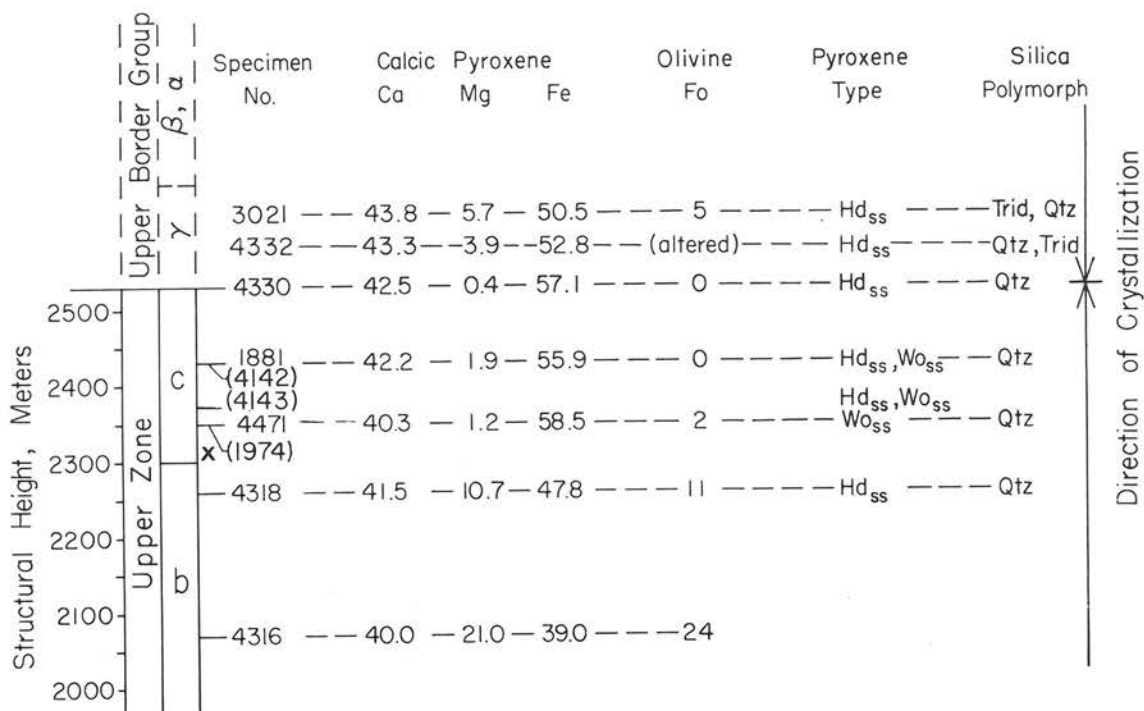


FIG. 1. Schematic representation of part of the Upper Zone and Upper Border Group of the Skaergaard intrusion, showing distribution of specimens discussed in text. Compositions of calcic pyroxenes, expressed in atomic %, are from Brown and Vincent (1963, Table 1). X shows approximate position of layered equivalent of EG 3021. Hd<sub>ss</sub>, hedenbergite solid solutions; Wo<sub>ss</sub>, ferrowollastonite solid solutions, now inverted to green Hd<sub>ss</sub>; Qtz, quartz; Trid, quartz paramorphs after tridymite.

tain green pyroxene rimmed by or intergrown with the brown variety. Note that EG 4471 and 1881 are crystal accumulates, where EG 4330 probably represents a liquid. Photomicrographs showing the pyroxenes from these three

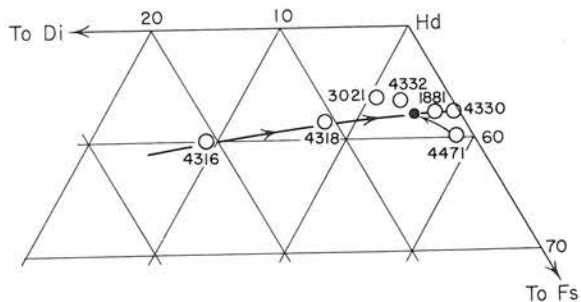


FIG. 2. Compositions of calcium-rich pyroxenes from the late stages of fractionation of the Skaergaard intrusion (Brown and Vincent, 1963, Fig. 2). EG 3021 and 4332 are from Upper Border Group  $\gamma$ ; the remainder are from the layered series (Upper Zone b to c). The crystallization trend-line is based only on the latter. EG 4471 is believed to have inverted from a ferrowollastonite solid solution. The solid circle represents the likely composition of the host hedenbergite of EG 4471 after exsolution and inversion. Because inversion took place shortly after crystallization (see Brown and Vincent, 1963, p. 186-190) the filled circle probably approximates the composition of the (hypothetical) Hd<sub>ss</sub> that would have been found in EG 4471 had Wo<sub>ss</sub> not been temporarily stable.

rocks are given in Figure 3. Chemical analysis of the pyroxenes are given in Brown and Vincent (1963, Table 1). Analyses of similar examples of inverted ferrous wollastonites are also given by Muir (1951), his EG 1974 being comparable with EG 4471, and his EG 4131 being intermediate between EG 4471 and EG 1881. (Structural heights given for Muir's specimens have been revised by Wager and Brown, 1968.)

The cumulate rocks from Upper Zone c all contain cumulus fayalitic olivine and intercumulus quartz. Rocks immediately overlying this zone (Upper Border Group  $\gamma$ , approximately 100 m thick) contain quartz paramorphs after tridymite, coexisting with primary quartz (for example, EG 3021, Fig. 4). If both pairs of minerals—Hd<sub>ss</sub>-Wo<sub>ss</sub> and quartz-tridymite—occurred in the same layer, then at some time during its crystallization history that layer must have been at a pressure and temperature corresponding to the intersection of the appropriate inversion curves in  $P$ - $T$  space. At the coexisting pairs occur at slightly different levels, an estimate of the pressure and temperature differences between the two levels will indicate how close the crystallization sequence came to the region of intersection.

Specimen EG 3021 occurs less than 100 m above EG 4330 and 200 m above EG 1881, corresponding to maximum pressure differences of about 30 and 60 bars, respectively. Crystallization at each level took place over a

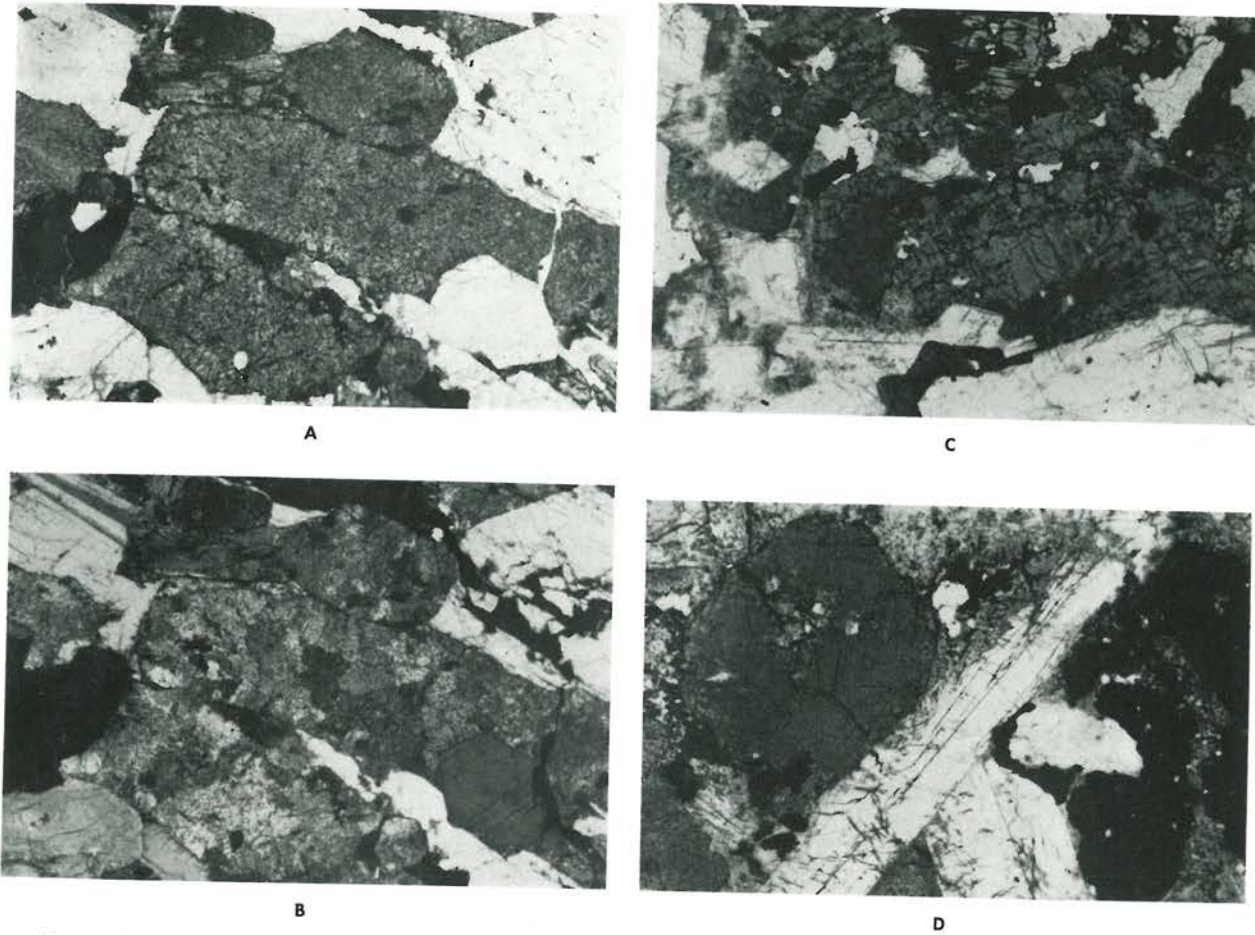


FIG. 3. Ferrohedenbergites from the Skaergaard intrusion. Reproduced by kind permission of the Clarendon Press, Oxford. A. Discrete cumulus crystals presumed to have been originally,  $Wo_{ss}$ . Each of the three crystals in the center of the photomicrograph has inverted to a mosaic of small  $Hd_{ss}$  crystals (see B). Specimen EG 4471.  $\times 17$ . B. Same as A, under crossed polars. C. Large poikilitic crystals of pale green  $Hd_{ss}$  with irregular rims and marginal patches of brown  $Hd_{ss}$ . The green pyroxene has been analyzed (no. 14, Table 1, and Figs. 1-3, Brown and Vincent, 1963), while the brown variety is believed equivalent to that found in later-crystallized rocks. Specimen EG 1881.  $\times 20$ . D. Crystal of brown  $Hd_{ss}$ , with a very narrow rim of late-stage material (amphibole and pale green pyroxene), from the latest differentiate of the Skaergaard layered series. Specimen EG 4330, 50.  $\times 20$ .

temperature range, or course, but it is nevertheless meaningful to estimate differences in the temperatures at which the clinopyroxene now present in each layer first crystallized or, say, at which fifty percent of the pyroxene had crystallized in each layer. We may refer to these as "average" temperature differences. An estimate of the "average" temperature difference between EG 1881 and EG 3021 may be made as follows. On the basis of the compositions of clinopyroxene and of olivine, EG 3021 probably crystallized at about the same time, and hence over approximately the same temperature interval, as rocks in the layered series between EG 4318 and EG 4471 (Fig. 1). Tilley, Yoder, and Schairer (1963, p. 78, 80; 1964, p. 94) determined the liquidus temperatures and temperatures of first appearance of  $Wo_{ss}$  (or  $Hd_{ss}$ ) in two Skaergaard specimens that have approximately the same stratigraphic separation as do EG

1881 and the layered equivalent of EG 3021 (see Fig. 1). For specimen EG 4472 (same level as EG 4471) the temperatures are: liquids,  $1035^{\circ}C$ ; first appearance of  $Hd_{ss}$  and  $Wo_{ss}$   $1010^{\circ}C$ . For EG 4330, the liquidus is at  $1020^{\circ}C$  and the first appearance of  $Hd_{ss}$  and  $Wo_{ss}$  at  $995^{\circ}C$ . The difference in liquidus temperatures, and also the difference in the temperatures of first appearance of  $Hd_{ss} + Wo_{ss}$ , is  $15^{\circ}C$ . Thus a reasonable estimate of the "average" temperature difference between EG 1881 and EG 3021 is  $15^{\circ}C$ ;  $30^{\circ}C$  would be a maximum difference. These experiments were performed in vacuum, and the temperatures determined may differ somewhat from those that prevailed *at pressure* in nature; however, the temperature differences at pressure were probably similar to those obtained in vacuum. Note that the liquidus temperature for EG 4472 must be a maximum inasmuch as that specimen is

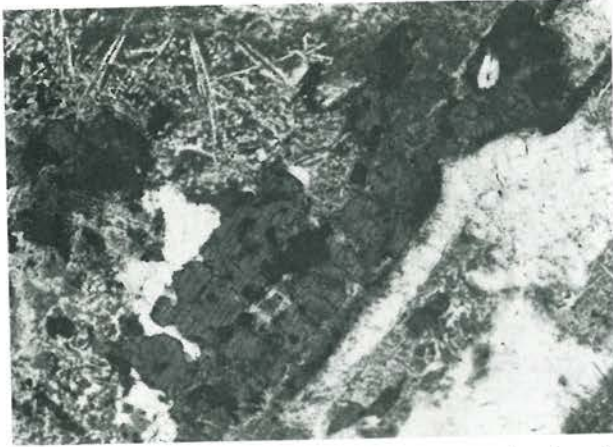


FIG. 4. Photomicrograph of specimen EG 3021, showing acicular crystals of quartz that are believed to have inverted from tridymite. Anhedral quartz crystals, products of direct precipitation from the magma, are also present in his specimen. Reproduced by kind permission of the Clarendon Press, Oxford.  $\times 20$ .

a crystal accumulate and therefore did not crystallize from a liquid of its own bulk composition. We conclude that the pressure and "average" temperature differences between EG 1881 and EG 3021 were not more than 60 bars and  $30^{\circ}\text{C}$ , respectively. Therefore, the intersection in pressure-temperature space of the quartz-tridymite and  $\text{Hd}_{\text{ss}}\text{-Wo}_{\text{ss}}$  inversions should give a close estimate of the pressure and temperature during crystallization of the late stages of the Skaergaard intrusion.

#### PREVIOUS EXPERIMENTAL WORK ON THE $\text{Hd}_{\text{ss}}\text{-Wo}_{\text{ss}}$ INVERSION

The pioneering study on synthetic Ca-Fe pyroxenes was made by Bowen, Schairer, and Posnjak (1933). Their discovery that hedenbergitic pyroxenes invert to  $\text{Wo}_{\text{ss}}$  upon heating to temperatures well below the metasilicate solidus was the basis for Wager and Deer's conclusion that the mottled green ferrohedenbergites from the Skaergaard intrusion had initially crystallized as ferro-wollastonite solid solutions. Bowen, Schairer, and Posnjak (1933, p. 213) showed an inversion loop between  $\text{Hd}_{\text{ss}}$  and  $\text{Wo}_{\text{ss}}$  with a minimum at approximately  $\text{Wo}_{32}\text{Fs}_{68}$  (mole %), and they indicated that the composition of  $\text{Hd}_{\text{ss}}$  coexisting with  $\text{Wo}_{\text{ss}}$  + fayalite + tridymite is about  $\text{Wo}_{25}\text{F}_{27}$ . Lindsley and Munoz (1969) redetermined the subsolidus relations for the join Hd-Fs using much longer run durations and hydrothermal experiments to demonstrate equilibrium. They found that only the hedenbergite-rich half of the  $\text{Hd}_{\text{ss}}\text{-Wo}_{\text{ss}}$  inversion loop of Bowen, Schairer, and Posnjak represents stable equilibrium and that the maximum solubility of  $\text{FeSiO}_3$  in  $\text{Hd}_{\text{ss}}$  and  $\text{Wo}_{\text{ss}}$  is somewhat less than that given by Bowen, Schairer, and Posnjak. A revised diagram for the join Hd-Fs, incorporating the subsolidus data of Lindsley and Munoz with the melting data of Bowen, Schairer, and Posnjak is given in Figure 5. At  $940^{\circ}\text{C}$ , faya-

lite and silica can coexist with  $\text{Hd}_{\text{ss}}$  ( $\text{Wo}_{40}\text{Fs}_{60}$ ) and  $\text{Wo}_{\text{ss}}$  ( $\text{Wo}_{38}\text{Fs}_{62}$ ). This result is consistent with the fact that the green, inverted  $\text{Wo}_{\text{ss}}$  is slightly richer in  $\text{FeSiO}_3$  than is the brown, primary  $\text{Hd}_{\text{ss}}$  from the Skaergaard intrusion (Muir, 1951, p. 708; Brown and Vincent, 1963, pp. 181, 183).

Yoder, Tilley, and Schairer (1963, p. 91) inverted ferrohedenbergites separated from Skaergaard specimens EG 4471, 4472, and 4143 to  $\text{Wo}_{\text{ss}}$  at  $970^{\circ} \pm 5^{\circ}\text{C}$  in evacuated tube experiments. They did not reverse the inversion, however, so their results give only a maximum temperature for the beginning of the inversion in vacuum.

Turnock has shown that the temperature of the  $\text{Hd}_{\text{ss}}\text{-Wo}_{\text{ss}}$  inversion strongly increases with increasing Mg-content for the join  $\text{Ca}_{0.5}\text{Mg}_{0.5}\text{SiO}_3\text{-Ca}_{0.5}\text{Fe}_{0.5}\text{SiO}_3$  (1962, p. 81) and the join  $\text{Ca}_{0.4}\text{Mg}_{0.6}\text{SiO}_3\text{-Ca}_{0.4}\text{Fe}_{0.6}\text{SiO}_3$  (personal communication, 1968). Compositions of late-stage  $\text{Hd}_{\text{ss}}$  from the Skaergaard intrusion lie close to the Fe-rich end of the latter join.

Lindsley (1967, p. 234) found that the temperature of the  $\text{Hd}_{\text{ss}}\text{-Wo}_{\text{ss}}$  inversion on the join Hd-Fs increases sharply with pressure. For example, pure hedenbergite inverts to  $\text{Wo}_{\text{ss}}$  at  $965^{\circ}\text{C}$  at one atmosphere but at approximately  $1200^{\circ}\text{C}$  at 10 kbars.

#### INVERSION OF GREEN FERROHEDENBERGITE FROM EG 4471

To locate an appropriate  $\text{Hd}_{\text{ss}}\text{-Wo}_{\text{ss}}$  inversion interval for the Skaergaard intrusion we have investigated the pressure-temperature relations for the green  $\text{Hd}_{\text{ss}}$  from EG

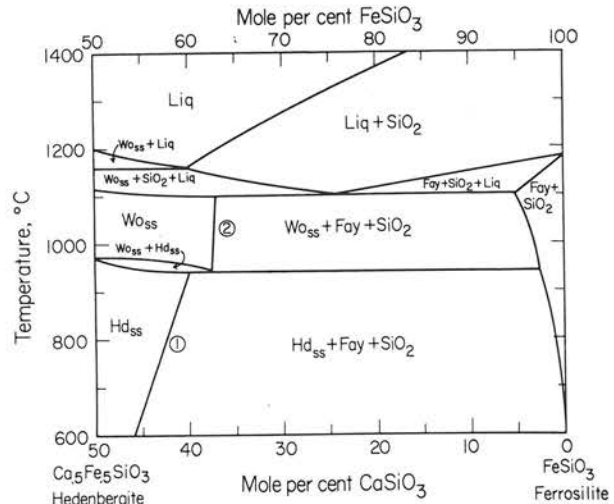


FIG. 5. Revised equilibrium diagram for the join hedenbergite-ferrosilite at low pressures (2 kbar and below) (Lindsley and Munoz, 1969). All liquids (Liq) contain small amounts of  $\text{Fe}_2\text{O}_3$ .  $\text{Wo}_{\text{ss}}$ , ferrous wollastonite solid solutions;  $\text{Hd}_{\text{ss}}$ , hedenbergite solid solutions; Fay, olivine close in composition to  $\text{Fe}_2\text{SiO}_4$ , but containing some  $\text{CaFeSiO}_4$ ;  $\text{SiO}_2$ , quartz or tridymite, depending on pressure and temperature. Curves 1 and 2 give the compositions of  $\text{Hd}_{\text{ss}}$  and  $\text{Wo}_{\text{ss}}$ , respectively, in equilibrium with fayalite +  $\text{SiO}_2$ .

4471 at pressures from 0 to 5 kbar. The starting material was a split of the mineral separate analyzed by Brown and Vincent (1963); part of the material was initially inverted to  $Wo_{ss}$  in vacuum at 1000°C to permit reversal of the reaction. Details of the experimental techniques employed and the experimental data are given in the Appendix. Our results are summarized in Figure 6.

We are uncertain of the exact nature of the transition from primary  $Wo_{ss}$  to  $Hd_{ss}$  in EG 4471. There are several possibilities: (1) Transition of  $Wo_{ss}$  to  $Hd_{ss}$  of the same composition; this is a true inversion, and will take place over a temperature interval. (2) Reaction of  $Wo_{ss}$  to  $Hd_{ss} + Fay + Qtz$ ; in the Hd-Fs system (Fig. 5) this reaction is univariant and takes place isothermally, but in the Mg-bearing natural system it must also take place over a temperature interval. (3) Reaction of  $Wo_{ss}$  to  $Hd_{ss} + FeSiO_3$ -rich pyroxene. Bown and Gay (1960, p. 386) found that the green  $Hd_{ss}$  of EG 1974 and EG 1881 are single phases, but that of EG 4143 shows exsolution of  $FeSiO_3$ -rich clinopyroxene. This metastable reaction also would take place over a temperature interval. We cannot tell which of these three processes took place in nature or in our experiments, but in keeping with past usage we will refer to the transition as an inversion, and to the necessary temperature interval as an inversion interval.

The inversion interval shown in Figure 6 is applicable directly only to the green, inverted  $Wo_{ss}$  from EG 4471; later hedenbergites from the Skaergaard intrusion would presumably invert over a lower temperature range and earlier hedenbergites would invert, if at all, over a higher temperature range. However, it is possible qualitatively to relate other late-stage Skaergaard rocks to the diagram. EG 4471 originally precipitated  $Wo_{ss}$  and quartz, and is therefore shown in the  $P$ - $T$  region where those fields overlap. Because EG 1881 occurs later in the crystallization sequence and at a higher stratigraphic level than does EG 4471, it must have been precipitated over a lower temperature range and at a lower pressure. EG 1881 contains inverted  $Wo_{ss}$ , primary  $Hd_{ss}$ , and quartz, so it is shown in Figure 6 as lying in the quartz field and within the  $Wo_{ss} + Hd_{ss}$  field (the assumption being that the inversion interval for EG 1881 is not much different from that for EG 4471).

EG 4330, containing primary  $Hd_{ss}$  and quartz is still later in the crystallization sequence, and must have crystallized over a lower temperature interval and at a lower pressure than did EG 1881; the  $Hd_{ss}$  in EG 4330 formed below its own inversion interval and therefore below that shown for EG 4471 in Figure 6. Finally, because of its higher elevation, EG 3021 must have crystallized at still lower pressures; but the Fe/Mg ratios of its clinopyroxene and olivine reflect a higher temperature range than any of the other three samples. EG 3021 contains both inverted tridymite and primary quartz, so it must lie athwart the quartz-tridymite inversion curve and, from arguments already presented, must lie at temperatures not more than

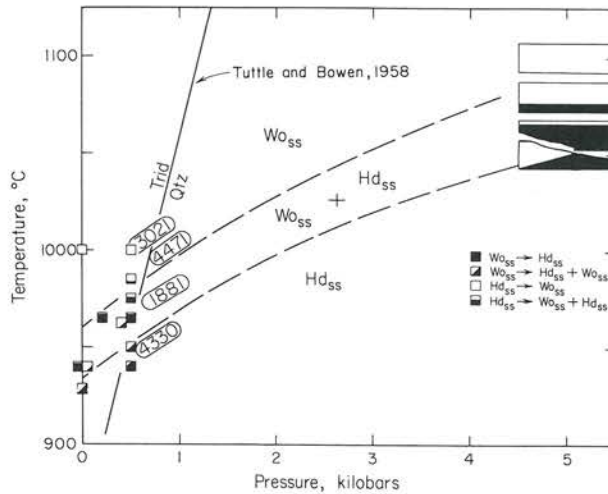


FIG. 6.  $Hd_{ss} = Wo_{ss}$  inversion for green pyroxene from specimen EG 4471, Skaergaard intrusion. Slow reaction rates prohibit exact determination of inversion interval, which is probably narrower than is shown. Amount of shading approximately proportional to amount of  $Hd_{ss}$  in run products.  $Wo_{ss}$ , ferri-ferrous wollastonite solid solution;  $Hd_{ss}$ , hedenbergite solid solution; Trid, tridymite; Qtz, quartz. Height of symbols reflects uncertainty in temperature of each experiment. Width of symbols reflects pressure uncertainty at 5 kbar but exaggerates the uncertainty at lower pressures.

The encircled numbers show schematically the inferred relations of samples EG 4471, 1881, 4330, and 3021 to the  $Hd_{ss}$ - $Wo_{ss}$  inversion curve for EG 4471 and to the quartz-tridymite inversion curve; see Fig. 1 for details of their stratigraphic relations. EG 3021 did not crystallize  $Wo_{ss}$  because the higher content of Mg stabilized clinopyroxene formation.

30°C above and at pressures not more than 60 bars below EG 1881. The distribution of pressures and temperatures shown in Figure 6 for these four rocks is the only one mutually consistent with the textural, mineralogical, and stratigraphic evidence, and with the available experimental data. We conclude that the rocks formed during the late crystallization stages of the Skaergaard intrusion (Upper Zone c and Upper Border Group  $\gamma$ ) crystallized at  $600 \pm 100$  bars and over a temperature interval that must have spanned the range 950–980°C.<sup>1</sup>

In Figure 6, EG 3021 falls in the  $Wo_{ss}$  field as determined for the inverted  $Wo_{ss}$  from EG 4471. It is necessary to pos-

<sup>1</sup> It is worth reemphasizing here that all the rocks crystallized over a temperature range: the temperatures indicated in Fig. 6 might well correspond to those at which approximately half the pyroxene now present in each rock had crystallized. Likewise, of the four specimens, only EG 4330 and EG 3021 crystallized at a fixed pressure. EG 1881 and EG 4471 are crystal accumulates, and the minerals now present in them crystallized over a possible pressure range that at a maximum corresponds to the thickness of the remaining magma through which they sank, that is, to the difference in elevation between each layer and its equivalent in the Upper Border Group. The pressure range cannot exceed approximately 85 bars for EG 4471 (based on a layer of liquid plus crystals with a maximum thickness of 280 m and a specific gravity of 3.0); for EG 1881 the pressure range is less.

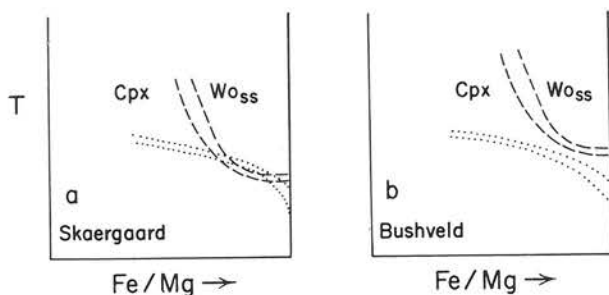


FIG. 7. Hypothetical and highly schematic diagrams showing the authors' interpretation of the relationship between the clinopyroxene (Cpx)- $Wo_{ss}$  inversion intervals and the crystallization curves for the Skaergaard and Bushveld magmas. Dotted lines: crystallization curves; approximate temperature range over which liquid of a given Fe/Mg ratio precipitated metasilicates. Dashed lines: approximate boundaries of Cpx- $Wo_{ss}$  inversion intervals. During the bulk of Skaergaard crystallization (a)  $Wo_{ss}$  was not stable. However, as the Fe/Mg ratio of the liquid increased with continuing fractionation, the crystallization curve intersected the Cpx ( $Hd_{ss}$ )- $Wo_{ss}$  inversion interval.  $Wo_{ss}$  was the only metasilicate precipitated (e.g., EG 4471, 1974) in the interval where the crystallization curve lay completely above the Cpx- $Wo_{ss}$  inversion. With increasing Fe/Mg ratio of the liquid Cpx and  $Wo_{ss}$  co-precipitated (for example, EG 4143, 1881) and finally only  $Hd_{ss}$  precipitated (EG 4330). According to this interpretation there should also be at least a narrow layer immediately underlying EG 4471 and 1974 in which Cpx and  $Wo_{ss}$  co-precipitated. Such a layer has not yet been reported.

The effect of increasing pressure on the temperatures of the Cpx- $Wo_{ss}$  inversion and of magmatic crystallization is unequal; the increase of the former is greater. Accordingly, in the Bushveld intrusion (b), which is thought to have crystallized at a higher pressure than did the Skaergaard intrusion, the crystallization curve never intersected the  $Wo_{ss}$  field.

tulate that the primary  $Hd_{ss}$  occurring in EG 3021 contains too much Mg for  $Wo_{ss}$  to have precipitated in its place. This conclusion is consistent with available experimental data on the Di-Hd join (Turnock, 1962) that the inversion temperature increases with increasing Mg/Fe ratio, and with the observation that the green, inverted  $Wo_{ss}$  contains less Mg than would a  $Hd_{ss}$  in the same position in the Skaergaard layered series (Muir, 1951, p. 708; Brown and Vincent, 1963, p. 181, 183). We tested this hypothesis by holding analyzed  $Hd_{ss}$  from EG 3021, 4332, and 4318, all of which contain somewhat more  $MgSiO_3$  than that from EG 4471 (Fig. 1), at 1000°C for 40 days in evacuated silica glass tubes. Also included in this experiment were the green, inverted  $Wo_{ss}$  from EG 4471 as a control; the brown, nearly Mg-free  $Hd_{ss}$  from EG 4330; and a pale green  $Hd_{ss}$  from the Bushveld intrusion whose composition (SA 1149, Wager and Brown, 1968, Table 28) is closely similar to that from EG 4330. The first three more magnesian samples failed to invert; the latter three did invert to  $Wo_{ss}$ , although SA 1149 inverted only partially. These results are not definitive; the failure of the three samples richest in Mg to invert suggests, but does not prove, that their  $Hd_{ss}$  was still stable. However, these experiments are consistent with our conclusion that only briefly during the crystallization history

of the Skaergaard intrusion were the activity of  $MgSiO_3$  and the pressure sufficiently low, while the temperature was sufficiently high, to permit primary precipitation of  $Wo_{ss}$ . In the Bushveld intrusion, on the other hand the pressure was too high to permit the precipitation of  $Wo_{ss}$  at any time. These interpretations are illustrated schematically in Figure 7.

We can determine a third intensive parameter that prevailed during these late stages of Skaergaard crystallization, the oxygen fugacity ( $f_{O_2}$ ), as follows: Specimen EG 1974 (= EG 4471) contains a titaniferous magnetite whose bulk composition (Vincent and Phillips, 1954, p. 12) recalculates to the binary composition  $Mt_{14.5}Usp_{85.5}$  (see Buddington and Lindsley, 1964, p. 314-328 for the justification of this recalculation). The experimental data show that the *maximum*  $f_{O_2}$  at which a spinel of this composition can be stable is  $10^{-13.6}$  bar at 950°C and  $10^{-13.0}$  bar at 980°C, the values for the wüstite-magnetite buffer (Buddington and Lindsley, 1964, Fig. 2, 5). An additional constraint results from the fact that EG 1974 contains fayalitic olivine and quartz as well as titaniferous magnetite. This assemblage defines the equilibrium oxygen fugacity through the relation:



and therefore

$$K_T = \frac{(a_{Fe_3O_4})^2 (a_{SiO_2})^3}{(a_{Fe_2SiO_4})^3 \cdot f_{O_2}}$$

where  $a_{Fe_3O_4}$  is the activity of  $Fe_3O_4$  in titaniferous magnetite, etc. The equilibrium constant  $K_T$  equals  $1/f_{O_2}$  when the activities of all the solid phases are unity, and it can be evaluated from the data of Eugster and Wones (1962, p. 90):  $K_T = 10^{11.97}$  at 950°C and  $10^{11.45}$  at 980°C. The activities of the solid phases are estimated as follows: As a first approximation the activity of  $Fe_3O_4$  is taken as equal to the mole fraction 0.145; note that any departure from ideality is likely to be positive since the  $Fe_3O_4$ - $Fe_2TiO_4$  series has a miscibility gap at lower temperatures. The coexisting olivine in EG 1974 contains 98 percent  $Fe_2SiO_4$  (Fig. 1), so to a good approximation  $a_{Fe_2SiO_4} = 0.98$ . Quartz apparently was not a cumulus phase in EG 1974, but inasmuch as it is a fairly abundant intercumulus phase, the activity of silica must have been essentially unity during precipitation of the olivine and titaniferous magnetite. Using these estimates we calculate the  $f_{O_2}$  at 600 bars as  $10^{-13.6}$  bar at 950°C and  $10^{-13.1}$  bar at 980°C. These must be *minimum* values, since any positive deviation from ideality of  $a_{Fe_3O_4}$  would yield higher values for  $f_{O_2}$ . This close correspondence between the calculated maximum and minimum values probably owes at least as much to good fortune as to experimental virtuosity. Nevertheless it is reasonable to conclude that the oxygen fugacity during the late stages of Skaergaard fractionation ranged from approximately  $10^{-13.0}$  (at 980°C) to  $10^{-13.6}$  bar (at 950°C) which happen to coincide with the values for the wüstite-magnetite buffer.

Evidently conditions became oxidizing relative to that

buffer at lower temperatures, since the titaniferous magnetite from EG 1974 contains ilmenite lamellae. On the basis of co-existing ilmenite and titaniferous magnetite in EG 4142 (= EG 1881), Buddington and Lindsley (1964, p. 331) derived a temperature of  $890 \pm 50^\circ\text{C}$  and an  $f_{\text{O}_2}$  of  $10^{-13.2 \pm 1.0}$ , conditions that probably reflect the cessation of granule-"exsolution" of ilmenite upon oxidation of the magnetite (p. 322-324). Although this value of  $f_{\text{O}_2}$  is numerically similar to that calculated above for EG 1974, it is oxidizing relative to the wüstite-magnetite buffer since it obtained at a lower temperature.

We do *not* conclude from these results that the entire Skaergaard intrusion crystallized under conditions of constant oxygen fugacity. Rather, we visualize crystallization of all but a minute fraction of this notoriously "dry" intrusion at oxygen fugacities whose numerical values were similar to those of the wüstite-magnetite buffer. Below  $950^\circ$ , however, only minute amounts of liquid remained, and the activity of the dissolved water increased accordingly. Under these conditions the activity of hydrogen would also increase (see, for example, Eugster and Wones, 1962, Fig. 3). Hydrogen would therefore tend to escape preferentially by thermal diffusion, and the system would become more oxidizing (Presnall, 1966, p. 778-779; Buddington and

Lindsley, 1964, p. 321). Because of a high molecular proportion of oxide phases to water, the extent of oxidation was not great. For example, of five titaniferous magnetite-ilmenite pairs from the Skaergaard intrusion, all indicate oxygen fugacities above those of the wüstite-magnetite buffer but still below those of the fayalite-magnetite-quartz assemblage (Buddington and Lindsley, 1964, p. 331).

Stoichiometric water is oxidizing with respect to the wüstite-magnetite buffer; at temperatures near  $950^\circ\text{C}$  and total pressures of 600 bars or less, a H-O fluid in equilibrium with the wüstite-magnetite buffer has a  $\text{H}_2/\text{H}_2\text{O}$  ratio of approximately 1 : 8. If the late-stage rocks of the Skaergaard intrusion exchanged oxygen isotopes with large volumes of meteoric groundwater (which would be essentially stoichiometric and hence oxidizing) as suggested by Taylor (1968, p. 60-62), most of the exchange must have taken place at temperatures below approximately  $950^\circ\text{C}$ .

## ACKNOWLEDGMENTS

We thank F. R. Boyd, W. C. Luth, and D. Smith for constructive criticism of the manuscript.

## APPENDIX

*Experimental techniques and data.* The results of critical experiments on the  $\text{Hd}_{\text{ss}}-\text{Wo}_{\text{ss}}$  inversion are given in Table 1. Three

TABLE 1. CRITICAL EXPERIMENTS ON INVERTED  $\text{Wo}_{\text{ss}}$  FROM EG 4471

| Run <sup>a</sup><br># | Pressure <sup>b</sup> | Temp. <sup>c</sup><br>°C | Duration |       | Buffer <sup>d</sup> | Starting<br>Material                            | Products <sup>e</sup>   |
|-----------------------|-----------------------|--------------------------|----------|-------|---------------------|---|---|
|                       |                       |                          | Days     | Hours |                     |   |   |
| 5                     | 5 kbar                | 1100                     | 0        | 4     | "Fe"                | $\text{Hd}_{\text{ss}}$                         | $\text{Wo}_{\text{ss}} + 2-3\% \text{Hd}_{\text{ss}}$         |
| 2                     | 5 kbar                | 1080                     | 0        | 16    | "Fe"                | $\text{Hd}_{\text{ss}}$                         | 80% $\text{Wo}_{\text{ss}}$ ; rest $\text{Hd}_{\text{ss}}$    |
| 4                     | 5 kbar                | 1060                     | 0        | 15    | "Fe"                | $\text{Hd}_{\text{ss}}$                         | 5-10% $\text{Wo}_{\text{ss}}$ ; rest $\text{Hd}_{\text{ss}}$  |
| 7                     | 5 kbar                | 1050                     | 0        | 18    | "Fe"                | $\text{Wo}_{\text{ss}} + \text{Hd}_{\text{ss}}$ | All $\text{Hd}_{\text{ss}}$                                   |
| 8                     | evac.                 | 1000                     | 3        | 0     | —                   | $\text{Hd}_{\text{ss}}$                         | All $\text{Wo}_{\text{ss}}$                                   |
| 11                    | evac.                 | 940                      | 33       | 2     | —                   | $\text{Wo}_{\text{ss}}$                         | 10% $\text{Hd}_{\text{ss}}$ ; rest $\text{Wo}_{\text{ss}}$    |
| 12                    | evac.                 | 940                      | 33       | 2     | —                   | $\text{Hd}_{\text{ss}}$                         | 5-10% $\text{Wo}_{\text{ss}}$ ; rest $\text{Hd}_{\text{ss}}$  |
| 14                    | evac.                 | 930                      | 26       | 2     | —                   | $\text{Wo}_{\text{ss}}$                         | 30% $\text{Hd}_{\text{ss}}$ ; rest $\text{Wo}_{\text{ss}}$    |
| 20                    | 200 bar               | 965                      | 1        | 22    | FMQ                 | $\text{Hd}_{\text{ss}}$                         | 3-5% $\text{Wo}_{\text{ss}}$ ; rest $\text{Hd}_{\text{ss}}$   |
| 25                    | 400 bar               | 960                      | 1        | 19    | FMQ                 | $\text{Wo}_{\text{ss}}$                         | 30% $\text{Hd}_{\text{ss}}$ ; rest $\text{Wo}_{\text{ss}}$    |
| 27                    | 500 bar               | 1000                     | 0        | 7     | FMQ                 | $\text{Hd}_{\text{ss}}$                         | $\text{Wo}_{\text{ss}}$ (+5% glass)                           |
| 18a                   | 500 bar               | 985                      | 0        | 20    | FMQ                 | $\text{Hd}_{\text{ss}}$                         | 60-70% $\text{Wo}_{\text{ss}}$ ; rest $\text{Hd}_{\text{ss}}$ |
| 18b                   | 500 bar               | 985                      | 0        | 27    | FMQ                 | (18a)   | 90-95% $\text{Wo}_{\text{ss}}$ ; rest $\text{Hd}_{\text{ss}}$ |
| 17a                   | 500 bar               | 975                      | 0        | 22    | FMQ                 | $\text{Hd}_{\text{ss}}$                         | 5% $\text{Wo}_{\text{ss}}$ ; rest $\text{Hd}_{\text{ss}}$     |
| 17b                   | 500 bar               | 975                      | 0        | 18    | FMQ                 | (17a)   | 15% $\text{Wo}_{\text{ss}}$ ; rest $\text{Hd}_{\text{ss}}$    |
| 15                    | 500 bar               | 965                      | 0        | 20    | FMQ                 | $\text{Hd}_{\text{ss}}$                         | 3-5% $\text{Wo}_{\text{ss}}$ ; rest $\text{Hd}_{\text{ss}}$   |
| 21a                   | 500 bar               | 965                      | 0        | 17    | FMQ                 | $\text{Wo}_{\text{ss}}$                         | 5-10% $\text{Hd}_{\text{ss}}$ ; rest $\text{Wo}_{\text{ss}}$  |
| 21b                   | 500 bar               | 965                      | 1        | 18    | FMQ                 | (21a)   | 50% $\text{Hd}_{\text{ss}}$ ; rest $\text{Wo}_{\text{ss}}$    |
| 26                    | 500 bar               | 955                      | 2        | 0     | FMQ                 | $\text{Hd}_{\text{ss}}$                         | All $\text{Hd}_{\text{ss}}$                                   |
| 22a                   | 500 bar               | 950                      | 0        | 16    | FMQ                 | $\text{Wo}_{\text{ss}}$                         | 20% $\text{Hd}_{\text{ss}}$ ; rest $\text{Wo}_{\text{ss}}$    |
| 22b                   | 500 bar               | 950                      | 2        | 23    | FMQ                 | (22a)   | 70% $\text{Hd}_{\text{ss}}$ ; rest $\text{Wo}_{\text{ss}}$    |
| 24                    | 500 bar               | 940                      | 1        | 20    | FMQ                 | $\text{Wo}_{\text{ss}}$                         | 70% $\text{Hd}_{\text{ss}}$ ; rest $\text{Wo}_{\text{ss}}$    |

<sup>a</sup> Run #: "a" and "b" refer to experiments in which the run material is recycled; that is, reacted further at the same pressure and temperature.

<sup>b</sup> Pressure: 5 kbar, dry, or "load" pressure (piston-and-cylinder device); evac, experiment in evacuated silica-glass tube; 200, 400, 500 bar, water pressure (Tuttle press).

<sup>c</sup> Temperature: 5 kbar,  $\pm 10^\circ\text{C}$ ; evac and hydrothermal,  $\pm 5^\circ\text{C}$ .

<sup>d</sup> Buffer: 5 kb, "Fe", represents equilibrium with metallic iron (essentially fayalite-iron-quartz buffer); evac, no external buffer; hydrothermal, fayalite-magnetite-quartz buffer.

<sup>e</sup> Products: percentages from visual estimates of optical mounts, corroborated by peak heights on X-ray diffractometer charts.  $\text{Hd}_{\text{ss}}$ , hedenbergite solid solution.  $\text{Wo}_{\text{ss}}$ , ferriiferous wollastonite solid solution.

types of apparatus (evacuated tubes, Tuttle press, and piston-and-cylinder; see Lindsley and Munoz, 1969, for descriptions) were employed to make the experiments, and in each a different method was used to control the oxidation state of the iron.

1. For very low-pressure experiments the charges were wrapped in  $\text{Ag}_{70}\text{Pd}_{30}$  foil and then sealed in evacuated silica-glass tubes. The solubility of iron in the silver-palladium alloy is very low under these conditions (Muan, 1963), and the foil prevents reaction between the charge and the silica tube.

2. For 200- to 500-bar experiments the charges were sealed in  $\text{Ag}_{50}\text{Pd}_{50}$  capsules with 5 to 10 percent water by weight; these capsules were then sealed in larger gold capsules together with a fayalite-magnetite-quartz (or tridymite) buffer plus water. Because EG 4471 contains quartz, fayalite, and titaniferous magnetite, the  $f_{\text{O}_2}$  imposed by the buffer must be reasonably close to that prevailing during precipitation of the inverted  $\text{Wo}_{\text{ss}}$ .

3. For experiments at 5 kbar the charges were confined in metallic iron capsules. Some reaction between ferric iron in the charge (1.25 wt %) and the iron capsule undoubtedly took place, with a resulting increase in the FeO content of the charge from 30.79 to 32.5 weight percent if all the ferric iron reacted. The resulting  $f_{\text{O}_2}$  would approximate that of the fayalite-iron-quartz buffer, well below that of methods 1 and 2, but similar to that of many experiments on synthetic pyroxenes in equilibrium with metallic iron. The slight change in bulk composition, combined with the pressure uncertainties in the solid-media, piston-and-cylinder apparatus at 5 kbar, requires that the 5-kbar results be used with caution.

Ideally the experiments should recreate as closely as possible the natural environment in which the green  $\text{Hd}_{\text{ss}}$  from EG 4471 originally inverted from  $\text{Wo}_{\text{ss}}$ . Not only the pressure and temperature, but the chemical potentials of all the constituents of the parent rock should be duplicated. With one major exception, the excess of water, our experiments at 200 and 500 bars probably met this specification reasonably well: however carefully made, mineral separates always contain minor amounts of the other minerals present in the rock. Inasmuch as it is the *presence* of these phases, rather than their abundance, that controls the chemical potentials, the  $\text{Hd}_{\text{ss}}$  and  $\text{Wo}_{\text{ss}}$  should have experienced a similar environment of *intensive* parameters in nature and in our experiments. Despite abundant evidence that the Skaergaard magma had a very low water content, we chose to use water as a pressure medium and a catalyst on the assumption that a high activity of water would not affect the  $\text{Hd}_{\text{ss}}\text{-Wo}_{\text{ss}}$  equilibrium. This assumption seems justified on the grounds that neither the clinopyroxene nor the pyroxenoid structure is likely to accept much water of OH, and no hydrous phases were formed. (Sclar, Carrison, and Stewart, 1968, have reported the synthesis of hydrated magnesium orthosilicates that have pyroxene structures. Their experiments, however, involved different bulk compositions, much higher pressures, and lower silica activities from those reported here.)

The green inverted  $\text{Wo}_{\text{ss}}$  from specimen EG 4471, which coexists with fayalitic olivine ( $\text{Fa}_{98}$ ) and quartz, has a low Mg-content (1.2%  $\text{MgSiO}_3$ ). If the original  $\text{Wo}_{\text{ss}}$  had been Mg-free, its composition would have fallen on curve 2 in Figure 5, neglecting for the moment the effect of pressure. If stable equilibrium had been maintained upon cooling, the  $\text{Wo}_{\text{ss}}$  would have reacted to a  $\text{Hd}_{\text{ss}}$  lying on curve 1 (Fig. 5) plus fayalite and silica. Cooling under conditions of metastable equilibrium might have resulted in (a) reaction to  $\text{Hd}_{\text{ss}}$  plus (metastable) ferrosilite solid solution, or (b) inversion to a (metastable)  $\text{Hd}_{\text{ss}}$  of the same composition. In case (b) the inversion would have taken place over a temperature interval, whereas in the first two cases the inversion would have been isothermal. But in fact the inverted  $\text{Wo}_{\text{ss}}$  from EG 4471 contains Mg, and inasmuch as  $\text{Wo}_{\text{ss}}$  and  $\text{Hd}_{\text{ss}}$  coexisting at any given temperature have different Mg/Fe as well as Ca/Fe ratios, the inversion must take place over a

temperature interval. Bown and Gay (1960, p. 386) found from X-ray analysis that the green inverted  $\text{Wo}_{\text{ss}}$  from EG 4143 contains a trace of  $\text{FeSiO}_3$ -rich clinopyroxene. Brown and Vincent (1963, p. 190) noted that the inverted  $\text{Wo}_{\text{ss}}$  is "cloudy with an indeterminate material which may have been exsolved on inversion" and suggested that exsolution "of the small excess of  $\text{FeSiO}_3$ " may have been necessary to permit inversion of the  $\text{Wo}_{\text{ss}}$  over an inversion interval. The temperature range of the inversion as indicated in Figure 6 undoubtedly reflects this necessary temperature interval as well as experimental problems in achieving equilibrium. Presumably Skaergaard rocks that contain both green, inverted  $\text{Wo}_{\text{ss}}$  and brown, primary  $\text{Hd}_{\text{ss}}$  (for example, EG 1881, EG 4143) reflect crystallization within such a temperature interval.

*Quartz-tridymite inversion.* Application of experimental data on the quartz-tridymite inversion to the Skaergaard intrusion requires the following assumptions: (1) that the clusters of acicular quartz present in specimens such as EG 3021 originally crystallized as tridymite; (2) that the tridymite crystallized stably; (3) that the tridymite crystallized as a primary phase from the Skaergaard magma; and (4) that the quartz-tridymite inversion curve determined for the simple system  $\text{SiO}_2\text{-H}_2\text{O}$  is applicable to complex chemical environments. Assumption (1) is based on morphology of the acicular quartz, which is typical of tridymite and atypical of quartz (Fig. 4). Assumption (2) seems justified by the very slow cooling rate of the Skaergaard mass relative to the volcanic rocks in which tridymite may precipitate metastably. With regard to (3), Wager and Brown (1968, p. 54) tentatively suggested that the restriction of inverted tridymite to the Upper Border Group of the Skaergaard intrusion might have resulted from heating by the later Basistoppen sheet. However, the conclusion of Gay and Muir (1962, p. 577), that the occurrence of inverted tridymite reflects lower pressures prevailing during crystallization of the Upper Border Group, seems more plausible: it is unlikely that the Basistoppen sheet could have heated large portions of the Upper Group sufficiently to permit secondary formation of tridymite at pressures that would have prohibited magmatic precipitation of tridymite.

There is widespread disagreement as to whether tridymite is stable as a pure phase in the unary system  $\text{SiO}_2$  (see Rockett and Foster, 1967, for a summary of the controversy). It appears to be impossible to synthesize tridymite except in the presence of other components—such as alkalis or water; but whereas the Fenner-Roy school argues that the additional components merely catalyze the reaction to tridymite, the Flörke school maintains that the additional components actually stabilize tridymite by entering into its structure. If the latter were correct, then it is possible that the temperature of the quartz-tridymite inversion might vary, depending on the nature of the stabilizing substances, and assumption (4) would be invalid. Assumption (4) is valid, however, if the temperature of the quartz-tridymite inversion can be shown to be independent of the kind of components added, regardless of whether these components merely catalyze the inversion or cause it by stabilizing the tridymite structure. We had hoped to avoid this problem by determining the  $P\text{-}T$  inversion curve of quartz from EG 3021, since the same components that might have stabilized tridymite would still be present. Unfortunately, the quartz reacted with the coexisting feldspar remaining in the impure separate and with the water used as the pressure medium to produce liquid, and the quartz-tridymite inversion could not be observed. (We could have used an inert gas as a pressure medium, but then the inversion would probably have been too sluggish to detect.) We then added excess silica to glasses made from the quartz plus feldspar separated from EG 3021: natural quartz (from Lisbon, Maryland) to one lot; and pure silica glass, which was subsequently crystallized to tridymite by heating the mixture to 1350°C for six hours, to another



lot. With these starting materials we successfully duplicated Tuttle and Bowen's bracket at 4000 psi (276 bars) (1958, p. 30). At  $900^{\circ} \pm 5^{\circ}\text{C}$  tridymite partially inverted to quartz, and at  $925^{\circ} \pm 5^{\circ}\text{C}$  quartz partially inverted to tridymite, in each case in the presence of a water-rich, silica-feldspar liquid. This is not a conclusive experiment; it provides only the negative result that the presence of other components in addition to water did not in this case affect the quartz-tridymite inversion. Nevertheless, it provides permissive evidence that assumption (4) may be valid.

*Experimental difficulties.* The experiments were hampered by slow reaction rates. Evacuated tube experiments held at temperature for over 30 days may show only partial reaction. Our reversed point within the  $\text{Hd}_{ss}$ - $\text{Wo}_{ss}$  inversion interval at  $940^{\circ}\text{C}$  in vacuum is based on 33-day experiments. The higher temperature for the beginning of the  $\text{Hd}_{ss}$  to  $\text{Wo}_{ss}$  inversion in vacuum obtained by Yoder, Tilley and Schairer (1963, p. 91) is probably due to the shorter duration (7 days) of their experiments.

Hydrothermal experiments at 200 to 500 bars pressed the limits of the Tuttle (1948) press (with a pressure vessel of alloy R-41, heated by an external resistance furnace), and each point in Figure 6 represents a compromise between desirable run duration

and the time (12 to 72 hours) a pressure vessel would operate without failure. It was usually impossible, therefore, to let the reaction go to completion, even when the run material was recycled at pressure and temperature. Most experiments in which reaction took place yielded the two reaction products  $\text{Hd}_{ss} + \text{Wo}_{ss}$ , and the placement of boundaries for the inversion interval in Figure 6 is subjective. The lower boundary must lie below  $965^{\circ}\text{C}$  at 500 bars, for that is the lowest temperature at which  $\text{Hd}_{ss}$  even partially inverted to  $\text{Wo}_{ss}$ ; the failure of any  $\text{Wo}_{ss}$  to form in an experiment of similar duration and at the same pressure but with a temperature  $10^{\circ}\text{C}$  lower suggests but does not prove that the lower boundary lies above  $955^{\circ}\text{C}$ . At the same pressure the upper boundary must lie above  $965^{\circ}\text{C}$  but below  $1000^{\circ}\text{C}$  (see Table 1). We suspect, but cannot prove, that the inversion interval is narrower than is shown in Figure 6. The inversion interval for the appropriate composition in the synthetic  $\text{CaClO}_3$ - $\text{FeSiO}_3$  system at one atmosphere is so narrow that Bowen, Schairer, and Posnjak (1933, p. 218) were unable to detect it. Furthermore, the small deviation in the composition of the green, inverted  $\text{Wo}_{ss}$  (EG 4471) from the normal Skaergaard trend line (Fig. 2) suggests that the natural inversion interval is narrow in  $T$ - $X$  sections.

## REFERENCES

- BOWEN, N. L., J. F. SCHAIRER, AND E. POSNJAK (1933) The system  $\text{CaO-FeO-SiO}_2$ . *Amer. J. Sci.* **26**, 193-284.
- BOWN, M. G., AND P. GAY (1960) An X-ray study of exsolution phenomena in the Skaergaard pyroxenes. *Mineral. Mag.* **32**, 379-388.
- BROWN, G. M., AND E. A. VINCENT (1963) Pyroxenes from the late stages of fractionation of the Skaergaard Intrusion, East Greenland. *J. Petrology* **4**, 175-197.
- BUDDINGTON, A. F., AND D. H. LINDSLEY (1964) Iron-titanium oxide minerals and synthetic equivalents. *J. Petrology* **5**, 310-357.
- EUGSTER, H. P., AND D. R. WONES (1962) Stability relations of the ferruginous biotite, annite. *J. Petrology* **3**, 82-125.
- GAY, P., AND I. D. MUIR (1962) Investigation of the feldspars of the Skaergaard intrusion, eastern Greenland. *J. Geol.* **70**, 565-581.
- LINDSLEY, D. H. (1967) The join hedenbergite-ferrosilite at high pressures and temperatures. *Carnegie Inst. Wash. Year Book* **65**, 230-234.
- , AND J. L. MUNOZ (1969) Subsolidus relations along the join hedenbergite-ferrosilite. *Amer. J. Sci.* **267A**, 295-324.
- MUAN, ARNULF (1963) Silver-palladium alloys as crucible material in studies of low-melting iron silicates. *Amer. Ceram. Soc. Bull.* **42**, 344-347.
- MUIR, I. D. (1951) The clinopyroxenes of the Skaergaard intrusion, eastern Greenland. *Mineral. Mag.* **29**, 690-714.
- PRESNALL, D. C. (1966) The join forsterite-diopside-iron oxide and its bearing on the crystallization of basaltic and ultramafic magmas. *Amer. J. Sci.* **264**, 753-809.
- ROCKETT, T. J., AND W. R. FOSTER (1967) The thermal stability of purified tridymite. *Amer. Mineral.* **52**, 1233-1240.
- SCLAR, C. B., L. C. CARRISON, AND O. M. STEWART (1968) High-pressure synthesis and stability of hydroxylated orthoenstatite in the system  $\text{MgO-SiO}_2\text{-H}_2\text{O}$  (abstr.). *Trans. Amer. Geophys. Union* **49**, 356.
- TAYLOR, H. P., JR. (1968) The oxygen isotope geochemistry of igneous rocks. *Contrib. Mineral. Petrology* **19**, 1-71.
- TILLEY, C. E., H. S. YODER, JR., AND J. F. SCHAIRER (1963) Melting relations of basalts. *Carnegie Inst. Wash. Year Book* **62**, 77-84.
- , AND ——— (1964) New relations on melting of basalts. *Carnegie Inst. Wash. Year Book* **63**, 92-97.
- TURNOCK, A. C. (1962) Preliminary results on melting relations of synthetic pyroxenes on the diopside-hedenbergite join. *Carnegie Inst. Wash. Year Book* **61**, 81-82.
- TUTTLE, O. F. (1948) A new hydrothermal quenching apparatus. *Amer. J. Sci.* **246**, 628-635.
- , AND N. L. BOWEN, 1958, Origin of granite in the light of experimental studies in the system  $\text{NaAlSi}_3\text{O}_8\text{-KAlSi}_3\text{O}_8\text{-SiO}_2\text{-H}_2\text{O}$ . *Geol. Soc. Amer. Mem.* **74**, 153 p.
- VINCENT, E. A., AND ROY PHILLIPS (1954) Iron-titanium oxide minerals in layered gabbros of the Skaergaard intrusion, East Greenland. *Geochim. Cosmochim. Acta* **6**, 1-26.
- WAGER, L. R., AND G. M. BROWN (1968) *Layered Igneous Rocks*. Oliver and Boyd, Edinburgh and London, 588 p.
- , AND DEER, W. A. (1939) Geological investigations in East Greenland, III, Petrology of the Skaergaard intrusion, Kaugerdlungsuag, East Greenland. *Medd. Grønland* **105**, 355 p.
- YODER, H. S., C. E. TILLEY, AND J. F. SCHAIRER (1963) Pyroxenes and associated minerals in the crust and mantle. *Carnegie Inst. Wash. Year Book* **62**, 84-95.